Journal of Engineering, Project, and Production Management
2026, 16(4), 2025-269

Emergency Logistics Network Planning Based on Multi-Strategy Improved SSA

Yijia Gao[1] and Tingfen Gao[2]
[1] Lecturer, School of Economics and Management, Yunnan Vocational College of Mechanical and Electrical Technology, Kunming, 650201, China,
[2] Associate Professor, Office of Academic Affairs, Yunnan University of Finance and Economics, Kunming, 650221, China, E-mail: gaotingfengtf@outlook.com (corresponding author)

Project Management
Received November 12, 2025; revised April 23, 2026; May 7, 2026; accepted May 13, 2026
Available online May 29, 2026

Abstract: The occurrence of public health incidents and natural disasters has seriously affected people's daily lives. In emergency situations, supplies are often scarce, making it difficult to balance timeliness, cost, and demand urgency in emergency logistics planning. To enhance the SALP swarm algorithm (SSA), this study suggests an emergency logistics planning model based on several tactics. First, a multi-objective optimization model is constructed to minimize transportation time and total cost, and to maximize satisfaction of demand urgency. To balance the capacities of local exploitation and global exploration, the study employs a nonlinear, adaptive, inertial weighting mechanism. Additionally, it employs a Levy flight mechanism to increase the algorithm's ability to escape local optima and a backpropagation learning technique to improve the quality of the original population. Experiments indicated that the improved algorithm achieved optimal optimization accuracy (mean squared error reduced to 1×10^-100) after approximately 90 iterations. The second-best SALP swarm algorithm attained optimal optimization accuracy of 1×10^{-15}. During supply disruptions, the total cost of the improved SALP algorithm rose from the baseline value of USD 53480 to USD 58660 (an increase of USD 5180), which was lower than the USD 8820 increase observed in the whale optimization algorithm. The minimum relative unfairness of the improved algorithm was 0.083. After removing the nonlinear adaptive adjustment, the total logistics cost increased by USD 219,000. In summary, the proposed model can effectively enhance the coordination and planning capabilities of emergency logistics, reduce casualties and the occurrence of secondary disasters caused by material delays, and minimize economic losses.

Keywords: SALP swarm algorithm, Emergency logistics, Logistics network planning, Nonlinear adaptive, Demand urgency.

DOI 10.32738/JEPPM-2025-269

1. Introduction

Throughout human history, countless natural disasters and epidemics have occurred, with major catastrophes inflicting immense loss of life and property (Jalal et al, 2022). The 1970 Bora cyclone claimed between 300,000 and 500,000 lives in the Ganges Delta. The 1976 Tangshan earthquake, measuring 7.8 on the Richter scale, instantly leveled the city (Abideen et al., 2023). Regional emergency response systems are severely challenged during disaster relief and reconstruction due to limited materials, manpower, and deployment capacity. Emergency Logistics Networks (ELNs) enhance regional disaster response capacity (Chen and Cai, 2025; Huang et al., 2025). These networks must deliver the right supplies to the correct locations and to the right people at maximum speed, efficiency, and cost-effectiveness, minimizing loss of life and property while supporting post-disaster rescue and recovery efforts (Sun et al., 2022; Mu et al., 2023). However, existing ELN planning fails to effectively coordinate factors such as timeliness, cost-effectiveness, and urgency of demand.

To address the problem of emergency logistics planning, Ghasemi et al. (2022) proposed a novel scenario-based stochastic multi-objective location-allocation-routing model tailored for humanitarian relief logistics, which is characterized by high uncertainty. The model aimed to minimize the expected total cost while ensuring fairness in evacuation and the distribution of relief items, including goods and rescue personnel. For small-to-medium-scale problems, it employed an epsilon-constrained method for solution. Experiments revealed that the model could efficiently allocate resources and identify suitable pathways. Aloui et al. (2022) proposed a novel dual-objective mixed-integer linear

programming approach for logistics network planning decisions that incorporates environmental factors. This method analyzed scenarios with single objectives before employing an aggregation method for Multi-Objective Optimization (MOO). Experiments demonstrated that horizontal cooperation among suppliers could reduce both total logistics costs and carbon emissions. Ergün et al. (2023) proposed a novel game-theoretic model for emergency logistics planning to address post-disaster logistics challenges. Starting from post-earthquake logistics issues, the model developed a cooperative game framework and introduced a solution concept for maximizing the transfer of goods. It consisted of transportation planning, emergency supply reception and distribution, procurement and storage methods, and delivery modes. Experiments demonstrated the model's effectiveness in emergency logistics planning for food and samples. To address the rapid increase in infectious medical waste, Liu et al. (2022) proposed a novel reverse logistics planning network. This network introduced mobile processing centers into the reverse logistics network to conserve resources. From economic and environmental perspectives, they developed a collaborative model for reverse logistics site selection and route optimization involving multiple participants. They solved the model using an augmented ε-constrained method. Experiments demonstrated that this approach effectively reduced costs and infection risks. To address the convergence issues of the SALP swarm algorithm (SSA) in multimodal scenarios, Zhang et al. (2023) proposed an Improved SSA (ISSA). While differential evolution was used to improve the balance between global search and local reinforcement in SSA and to strengthen individual search skills, chaotic initialization produced a more ideal initial population. This approach was shown to be significantly better than the original SSA and other comparable techniques in experiments (Yao et al, 2023). Zhou and Zhang (2023) proposed an improved dual-objective SSA to enable green logistics vehicle scheduling and reduce path conflicts. By decomposing the dual-objective problem, the algorithm combined SSA with three operators employing random distributions to enhance and balance its exploration and exploitation capabilities.

In flexible contexts, experiments showed that the Improved Sparrow Search Algorithm (ISSA) more accurately balanced production efficiency with energy savings (Zhang et al., 2023). Abed-Alguni et al. (2022) proposed an ISSA to address the premature convergence issue of SSA. Laplace crossover operators were then used to enhance exploration, while a hybrid adversarial learning approach was finally applied to improve convergence speed and exploration efficiency. Experiments demonstrated that this algorithm significantly outperformed other methods in search effectiveness (Zhou and Zhang, 2023). Unlike the single improvement strategies referenced in the literature (Yao et al., 2023; Zhang et al., 2023; Zhou and Zhang, 2023), which addressed either algorithmic convergence or population diversity, this study integrates non-linear adaptive inertial weights, reverse learning initialization, and the Lévy Flight (LF) mechanism. This approach improved the SSA's global search capability while balancing dynamic constraints in the MOO of emergency logistics. It addressed the co-optimization challenge between demand urgency and fairness, a topic that has not been explored in previous research.

Existing research has examined Emergency Logistics Network (ELN) planning and SSA improvement from multiple perspectives, yielding certain results. However, the following limitations remain: (1) In model construction, Ghasemi et al. (2022) incorporated cost-expectation minimization into their stochastic programming model but did not introduce a dynamic assessment of demand urgency. (2) Regarding algorithmic enhancements, Zhang et al. (2023) improved SSA convergence through chaotic initialization and differential evolution. However, they did not address the uneven distribution of the Pareto frontier in MOO. (3) In application scenarios, Ergün et al. (2023) developed a game-theoretic model for post-earthquake logistics planning. However, the model's complexity limited its real-time applicability in practical emergency response scenarios. Therefore, this research proposes an emergency logistics planning network employing a multi-strategy ISSA. This method innovatively constructs an MOO model that balances timeliness and transportation costs. It then calculates demand urgency using the entropy-weighted Technique for Order of Preference by Similarity to Ideal Solution (TOPSIS) and incorporates this metric into the optimization model. The study integrates nonlinear adaptive inertial weighting, reverse learning initialization, and an Lévy Flight (LF) mechanism-enhanced SSA to solve the MOO model.

2. Materials and Methods

2.1. Multi-Objective Emergency Logistics Planning Model Construction

ELNs fundamentally differ from profit-driven commercial logistics, exhibiting characteristics such as suddenness, uncertainty, weak economic viability, high risk, and fluctuating demand. Emergency events are unpredictable in terms of their timing, location, scope, and nature. Requirements for the types and quantities of supplies vary significantly across different stages of an incident, while infrastructure such as roads and communications may become paralyzed (Abed-Alguni et al., 2022). Fig. 1 depicts the precise configuration of an ELN.

In Fig. 1, emergency logistics primarily encompasses four key nodes: procurement, transportation, warehousing, and distribution. Upon receiving emergency event information, the command center procures the corresponding supplies from suppliers, consolidates them at warehouse centers, and transports them to the emergency site. Upon arrival, supplies are delivered to secondary Distribution Points (DPs) for distribution to affected populations. If certain areas have sufficient supplies, they can be stored or transferred to other regions. Information can be collected at each node of the ELN and transmitted to the information center for unified coordination by the command center. The multi-objective ELN planning assumes the following conditions: (1) The transport network constitutes a fully connected graph. (2) Supplies are of a single, universal type. (3) Demand distribution conforms to a truncated normal distribution. (4) Path disruption probabilities are independent and identically distributed. In planning the ELN, the primary optimization objectives are minimizing time, minimizing cost, and prioritizing demand urgency. The minimum time function is expressed as in Eq. (1) (Malik and Suhag, 2022).

$$\min_{time} = \sum_{v\in V}\sum_{i\in I}\sum_{j\in J} T_{ijv} if_{ijv} + \sum_{u\in U}\sum_{j\in J}\sum_{n\in N} T_{jnu} if_{jnu} + \sum_{j\in J} T_j if_j \tag{1}$$

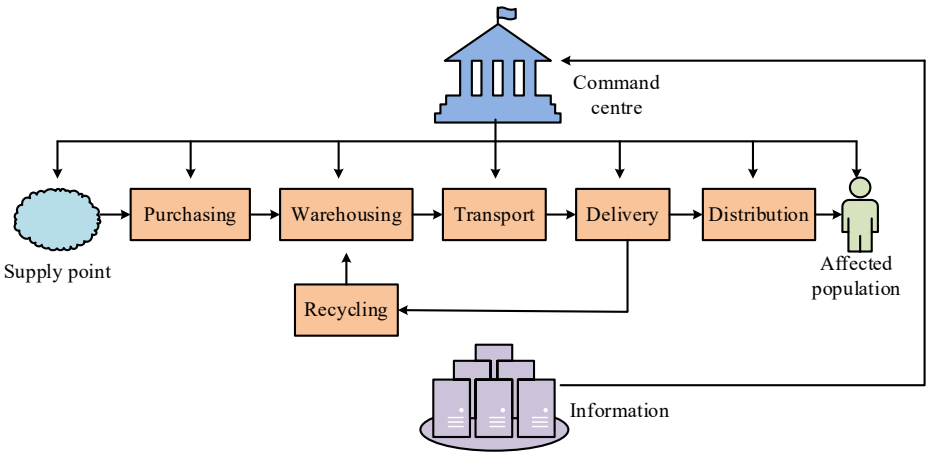

Fig. 1. Specific structure of the ELN

In Eq. (1), $\min_{time}$ denotes the shortest time for the ELN. V represents the set of vehicles from the Supply Point (SP) to the storage point. U denotes the set of vehicles from the storage point to the DP. I is the set of SPs. J is the set of storage points. N denotes the set of Distribution Points (DPs) . T_{ijv} indicates the transportation time using vehicle v from SP i to storage point j. if_{ijv} denotes the transportation time when vehicle passage conditions are met. T_{jnu} denotes the transportation time from the storage point j to DP n. if_{jnu} indicates the vehicle's possible condition from the storage point to the DP. T_j represents the time required to establish the storage point. if_j indicates whether establishing this storage point is necessary. The minimum cost includes two-level transportation costs and storage reduction costs. The transportation cost from the SP to the storage point is calculated as shown in Eq. (2) (Mahmood et al, 2022).

$$Cost_{IJ} = \sum_{i \in I} \sum_{j \in J} p(1-p) c_{ij} d_j \tag{2}$$

In Eq. (2), $Cost_{IJ}$ represents the total transportation cost from the SP to the warehouse point. p denotes the probability of Supply Point (SP) interruption. c_{ij} indicates the transportation cost from SP i to warehouse point j. d_j represents the demand volume at warehouse point j. The transportation cost from the warehouse point to the DP is calculated as shown in Eq. (3).

$$Cost_{JN} = \sum_{j \in J} \sum_{n \in N} q(1-q) c_{jn} d_n \tag{3}$$

In Eq. (3), $Cost_{JN}$ denotes the total transportation cost from the warehouse to the DP. q represents the interruption probability at the warehouse. c_{jn} indicates the transportation cost from warehouse j to DP n. d_n signifies the demand volume at the DP. If a new warehouse needs to be constructed, the Construction Cost (CC) is calculated as shown in Eq. (4) (Chukwuka et al., 2023).

$$Cost_j = f_j + e_j A_j \tag{4}$$

In Eq. (4), $Cost_j$ represents the CC of warehouse point j. f_j denotes the average daily CC of warehouse point j. e_j indicates the average daily CC per unit capacity of warehouse point j. A_j signifies the maximum storage capacity. During disasters, the severity of damage varies across regions, leading to differing levels of urgency in material demand. The study employs the entropy weight-TOPSIS method to calculate disaster demand urgency. First, a corresponding evaluation indicator system is constructed, as shown in Fig. 2.

In Fig. 2, the objective layer represents the urgency of material needs in disaster-affected areas, while the criterion layer encompasses three categories: population conditions, environmental factors, and material requirements. The first category of indicators includes the number of affected people, the proportion of vulnerable populations, and population density. The second category comprises the affected area, the extent of facility damage, the risk of secondary disasters, and regional weather conditions. The third category covers the severity of material shortages and the capacity of medical support. Eq. (5) illustrates that the study first determines the weights for each indication using the entropy-based approach (Zhang et al., 2022).

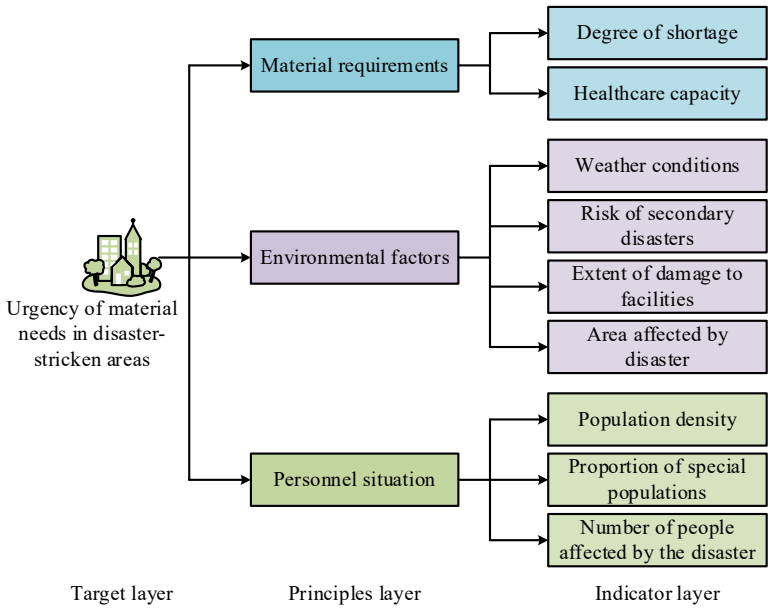

Fig. 2. Evaluation index system for the urgency of disaster relief needs

$$w_i = \beta_i / \sum_{n=1}^{N} \beta_i \tag{5}$$

In Eq. (5), w_i denotes the weight of the i th indicator. β_i represents the redundancy of the i th indicator. After calculating the indicator weights, the TOPSIS method is applied to compute proximity and perform ranking. First, the weighted standardized choice matrix is used to calculate the positive and negative ideal solutions (ISs), and then the distances to these ISs are calculated. Finally, proximity values are computed and ranked by magnitude. Proximity calculation is shown in Eq. (6).

$$\zeta_i = \frac{d_i^-}{d_i^+} + d_i^- \tag{6}$$

In Eq. (6), ζ_i represents the proximity of each DP. d_i^- is the negative IS. d_i^+ is the positive IS. The higher the proximity value of a DP, the greater the urgency of that region. In the emergency logistics planning model, the transportation volume from SPs must be no greater than the production volume, as shown in Eq. (7).

$$\sum_{j\in J}\sum_{v\in V} x_{ij}^v \le S_i \tag{7}$$

In Eq. (7), S_i represents the maximum production capacity of the SP. x_{ij}^v denotes the transportation volume of vehicle v from SP i to storage point j. Each storage center must also satisfy the flow balance constraint, ensuring that the total inflow of materials equals the total outflow to meet transshipment or storage requirements, as shown in Eq. (8).

$$\sum_{i\in I}\sum_{v\in V} x_{ij}^v = \sum_{n\in N}\sum_{u\in U} y_{jn}^u \tag{8}$$

In Eq. (8), y_{jn}^u represents the transport volume of vehicle u from storage point j to DP n. The flow balance constraint ensures that materials neither run short nor accumulate excess inventory at the storage center, and that all incoming materials are distributed to downstream DPs. The demand fulfillment constraint ensures that the total volume of materials shipped to each DP meets its assessed demand, the ultimate objective of emergency logistics, as shown in Eq. (9).

$$\sum_{j\in J}\sum_{v\in V} y_{jn}^u \ge D_n \tag{9}$$

In Eq. (9), D_n represents the material demand at DP n. After constructing the ELN planning model, the study requires normalization to eliminate dimensional effects. The study employs the Pareto front method to generate a set of non-inferior solutions (NISs), which are then ranked using the entropy-weighted TOPSIS approach. The solution with the highest overall proximity is selected as the planning scheme, thereby circumventing the subjective weighting bias inherent in weighted summation methods.

2.2. Multi-Strategy ISSA Problem Solving

The objective function and constraints in the ELN planning model are both nonlinear, making it a complicated multi-objective, multi-constraint optimization problem. SSA is exceptionally well-suited to handling such complex, nonlinear problems because it leverages the collective movement of the bottle-nose squid chain within the solution space to find optimal solutions. SSA can simultaneously address all objectives and constraints, yielding a satisfactory Pareto frontier or a comprehensive optimal solution (Tian et al., 2023). Individuals in SSA are categorized as leaders and followers. Leaders occupy the vanguard, guiding the swarm toward food sources, while followers movements are influenced solely by the preceding individual. The specific operational flow of SSA is illustrated in Fig. 3.

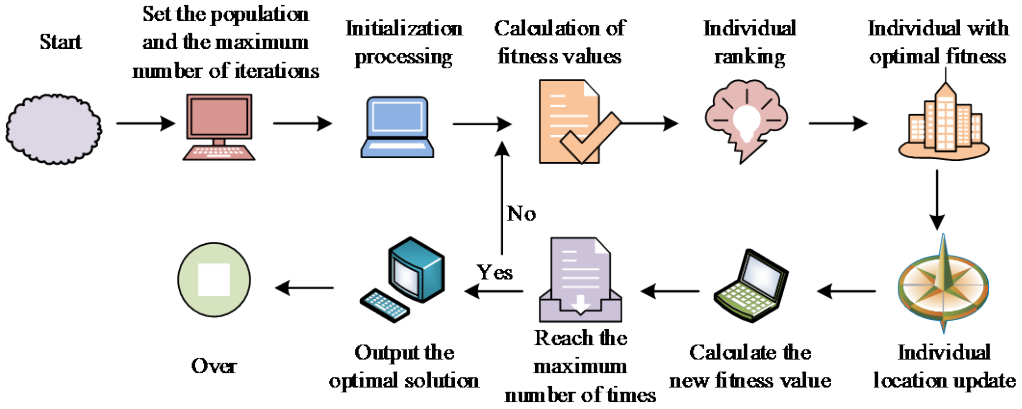

Fig. 3. Specific operational process of the Tsun-Hai-Shou algorithm

In Fig. 3(a), the population size and maximum iteration count are first set, followed by the initialization of the positions of all tunicate individuals. The initial Fitness Values (FVs) for all individuals are then calculated and sorted, with the individual possessing the optimal fitness serving as the current food source location. After completing the fitness calculation, the positions of the leader and follower individuals are updated, followed by the calculation of new FVs and food source locations. When the iteration count reaches the maximum iteration limit, the optimal solution is output. Otherwise, the process returns to the FV calculation step. Even though SSA offers several benefits, it is prone to getting stuck in local optima due to its small parameter set. This study improves it by employing a nonlinear adaptive inertia weight. In SSA, the update of follower particles is typically influenced by the inertia weight c. Conventional SSA sets c as a constant, making it difficult to balance global and local optimization (Dewangan and Saxena, 2023). Therefore, this study introduces nonlinear adaptive adjustment. At fewer iterations, a larger inertial weight c enables rapid global optimization. As iterations increase, a smaller inertial weight c enhances local optimization capabilities. The adjustment of inertial weight c is shown in Eq. (10).

$$c(t)=c(t_1)-\frac{4\left(c_{\max}-c(t_1)\right)}{(t_1-t_2)^2}t^2+\frac{4(t_1+t_2)\left(c_{\max}-c(t_1)\right)}{(t_1-t_2)^2}t-\frac{4t_1t_2\left(c_{\max}-c(t_1)\right)}{(t_1-t_2)^2} \tag{10}$$

In Eq. (10), $c(t)$ denotes the inertia weight after t iterations. $c_{\max}$ represents the maximum inertia weight. Among them, $t_1>t$ and $t_2<t$. In swarm intelligence algorithms, the more uniformly distributed the initial population is across the solution space, the higher the quality of the initial solutions, and the faster the solution speed. However, the initial population in SSA is typically randomly generated, resulting in unevenly distributed individuals that can slow down the solution process. Therefore, this study employs reverse learning to optimize the initial population. After randomly generating the initial population, a corresponding reverse population is generated based on it, as shown in Eq. (11).

$$X_j^i=rb_j+lb_j-X_j^i \tag{11}$$

In Eq. (11), X_j^i denotes the position of the individual i in the j dimension. rb_j and lb_j is the upper and lower bound of the search space. After generating the reverse population, the study merges the initial population with it. Those with the highest fitness rankings are selected to form the new population after Fitness Values (FVs) are calculated. A comparison between populations using conventional initialization and reverse learning initialization is shown in Fig. 4.

In Fig. 4(a), individuals from the standard initialization method cluster on both sides of the x-axis, with partial gaps between 0.4 and 0.6. In Fig. 4(b), populations from the reverse learning initialization exhibit greater uniformity, with tunicate individuals distributed across all regions, enabling faster discovery of initial solutions. To further enhance SSA's optimization accuracy and escape local optima, the study adopts a Levy walk-enhanced version of the leader-of-the-pack search. The large strides of Levy walk expand the search space and overcome local constraints, while numerous short-range steps enable thorough exploration of the surrounding area, thereby improving local exploration capabilities. The calculation of the Levy walk is shown in Eq. (12).

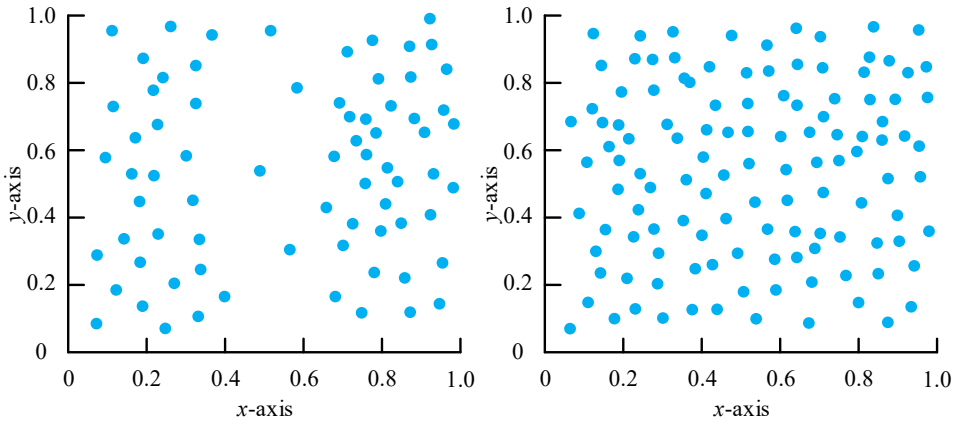

(a) Ordinary initialization (b) Reverse learning initialization

Fig. 4. Population comparison of conventional vs reverse learning initialization

$$Levy = \frac{1}{\pi}\int_0^{\infty} \exp\left(-\alpha|g|^{\alpha}\right)\cos(gs)dg \tag{12}$$

In Eq. (12), $Levy$ denotes the flight function. α represents the stable distribution parameter. g denotes the integral variable. To overcome the challenges of stride control and oscillatory convergence trajectories arising from the heavy-tailed nature of Levy walks, this study employs a multiplication operation between the random strides of Levy walks and a fixed stride scaling factor. The stride scaling factor acts as a global damper, systematically compressing the magnitude of all strides. This prevents futile searches caused by excessively large absolute stride values and constrains search behavior within a reasonable range. The random stride calculation for LF is shown in Eq. (13).

$$L = \frac{u'}{|v'|^{\frac{1}{\alpha}}} \tag{13}$$

In Eq. (13), L denotes the random stride of a LF. Both u' and v' represent random numbers that satisfy a normal distribution. The stochastic stride calculation process inherently incorporates a constraint mechanism introduced by the normally distributed random numbers u' and v'. This ensures that the generated strides have a stable distribution with a finite variance. This circumvents the risk of infinite variance inherent in the standard Lévy distribution. This guarantees that the volatility of the stochastic strides remains under control. The normal distribution is given by Eq. (14).

$$u' \square N\left(0,\delta_{u'}^2\right), v' \square N\left(0,\delta_{v'}^2\right) \tag{14}$$

In Eq. (14), N denotes the normal distribution. $\delta_{u'}$ is calculated as shown in Eq. (15).

$$\delta_{u'} = \left[\frac{\Gamma(1+\alpha)\cdot\sin\left(\frac{\alpha}{2}\pi\right)}{\Gamma\left(\frac{1+\alpha}{2}\right)\cdot 2^{\frac{\alpha-1}{2}}\alpha}\right] \tag{15}$$

In Eq. (15), Γ denotes the gamma function, and $\delta_{v'}$ equals 1. The improvement strategies do not operate in isolation but are integrated throughout the entire algorithmic iteration process, forming an effective synergy. Backward learning provides an excellent starting point for optimization, while the nonlinear adaptive inertial weight serves as a macro-level scheduler that controls the search rhythm. Meanwhile, controlled LF functions as a strike force, delivering crucial local breakthrough capabilities when the search stalls. These three components complement each other, collectively ensuring that the enhanced SSA converges to high-quality, satisfactory solutions faster, with higher precision, and with greater robustness. The ISSA ELN solution process is illustrated in Fig. 5.

In Fig. 5, the algorithm parameters and population are initialized, with corresponding start and end points set. The population is optimized using a reverse learning initialization method. The FVs of all individuals are computed, and leaders and followers are selected. When updating the leader's position, a nonlinear adaptive method is employed to adjust the inertia weight parameter. Concurrently, the LF is used to enhance the population leader's search behavior, promoting escape from local optima. Subsequently, the FVs of all individuals are recalculated to determine everyone's optimal position. When the maximum iteration count is reached, the optimal solution is output. Otherwise, the process repeats. The ISSA algorithm proposed in the study is itself a general MOO algorithm. Its core mechanisms (nonlinear adaptive inertia weight, reverse learning initialization, and Lévy flight) do not rely on the specific assumptions of emergency scenarios. Therefore, this method can also be applied to non-ELNs (e.g., commercial supply chains, cold chain logistics, and e-

commerce deliveries), requiring only corresponding adjustments to the objective function and constraints. Specifically, "maximizing demand urgency" can be replaced with "maximizing customer satisfaction" or "minimizing carbon emissions", the interruption probability can be replaced with conventional transportation reliability parameters, and the hard time window constraints can be removed, specific to emergency scenarios.

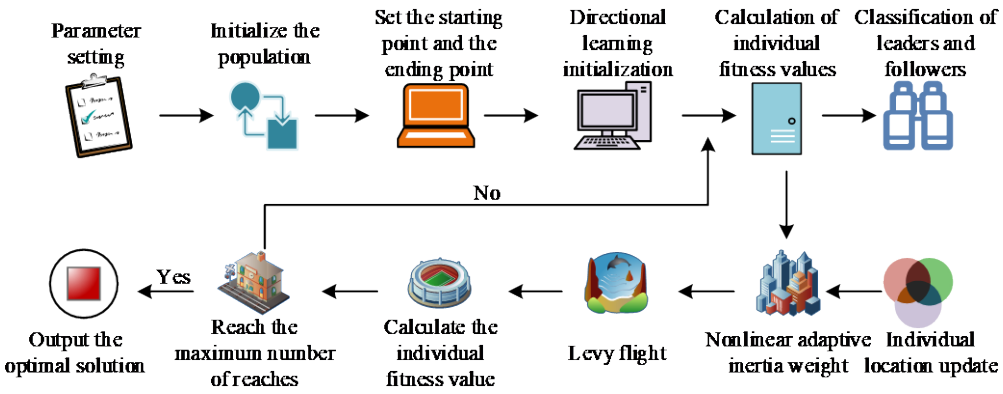

Fig. 5. ELN solution process using the ISSA

In Fig. 5, the algorithm parameters and population are initialized, with corresponding start and end points set. The population is optimized using a reverse learning initialization method. The FVs of all individuals are computed, and leaders and followers are selected. When updating the leader's position, a nonlinear adaptive method is employed to adjust the inertia weight parameter. Concurrently, the LF is used to enhance the population leader's search behavior, promoting escape from local optima. Subsequently, the FVs of all individuals are recalculated to determine everyone's optimal position. When the maximum iteration count is reached, the optimal solution is output. Otherwise, the process repeats. The ISSA algorithm proposed in the study is itself a general MOO algorithm. Its core mechanisms (nonlinear adaptive inertia weight, reverse learning initialization, and Lévy flight) do not rely on the specific assumptions of emergency scenarios. Therefore, this method can also be applied to non-ELNs (e.g., commercial supply chains, cold chain logistics, and e-commerce deliveries), requiring only corresponding adjustments to the objective function and constraints. Specifically, "maximizing demand urgency" can be replaced with "maximizing customer satisfaction" or "minimizing carbon emissions", the interruption probability can be replaced with conventional transportation reliability parameters, and the hard time window constraints can be removed, specific to emergency scenarios.

3. Results and Analysis

3.1. Performance Testing of Enhanced SSA

The experimental hardware configuration includes an Intel® Core™ i7-12700H processor running at 2.70GHz, an NVIDIA GeForce RTX 3070 GPU, 16GB of RAM, and a 1TB NVMe SSD for storage. In the software settings, the operating system is Windows 11 Pro 22H2. The population size for ISSA is set to 50, the maximum number of iterations is set to 300, the maximum inertia weight is set to 0.4, the leader proportion is set to 0.2, and the LF parameter is set to 1.5. The comparison algorithms employed in the experiment include standard SSA, Particle Swarm Optimization (PSO), and Genetic Algorithm (GA). The study selected two single-peak and two multi-peak test functions to evaluate the performance of the improved SSA algorithm. Detailed information on the different test functions is shown in Table 1.

Table 1. Details of test functions

	Function expression	Radius	Dimensionality	Optimal value
Single-peak test function	$F_1(x)=\sum_{i=1}^{n}x_i^2$	-80~80	30	0
	$F_2(x)=\sum_{i=1}^{n}\left(\left\lvert x_i+\frac{1}{2}\right\rvert\right)^2$	-80~80	30	0
Multi-peak test function	$F_3(x)=-\sum_{i=1}^{4}c_i\exp\left(-\sum_{j=1}^{3}a_{ij}(x_j-p_{ij})^2\right)$	1~5	3	0.024
	$F_4(x)=\sum_{i=1}^{n}\left(\sum_{j=1}^{i}x_j\right)^2$	-30~30	30	0

Note: The results of the parameter sensitivity analysis for the improved SSA are shown in Table 2.

In Table 2, the optimal parameter combination was (50/0.4/1.5), demonstrating the best balance of accuracy, convergence speed, and stability on both test functions F1 and F3. A population size of 20 may result in insufficient search

capability, while a size of 100 increases computational overhead. An inertia weight that was too low (0.2) restricted global exploration, while one that was too high (0.8) diminished local exploitation capability. An LF parameter of 1.5 achieved the optimal compromise between escaping local optima and ensuring convergence stability. Fig. 6 illustrates the performance of ISSA across various single-mode test functions.

Table 2. Sensitivity analysis of parameters for the improved SSA

Parameters (Population/maximum inertia weight/flight parameters)	Test function	Average optimization precision (log10)	Convergence iterations	Stability	Overall score
(50/0.4/1.5)	F1	-100	90	0.12	95.2
	F3	-22	150	0.18	91.8
(20/0.4/1.5)	F1	-85	120	0.25	78.3
	F3	-18	180	0.32	72.6
(100/0.4/1.5)	F1	-98	85	0.15	88.7
	F3	-21	145	0.2	86.9
(50/0.2/1.5)	F1	-92	110	0.22	82.1
	F3	-19	170	0.28	79.4
(50/0.8/1.5)	F1	-88	130	0.35	75.6
	F3	-16	190	0.41	70.8
(50/0.4/1.0)	F1	-95	100	0.18	85.3
	F3	-20	160	0.25	83.7
(50/0.4/2.0)	F1	-90	125	0.3	77.9
	F3	-17	185	0.38	73.2

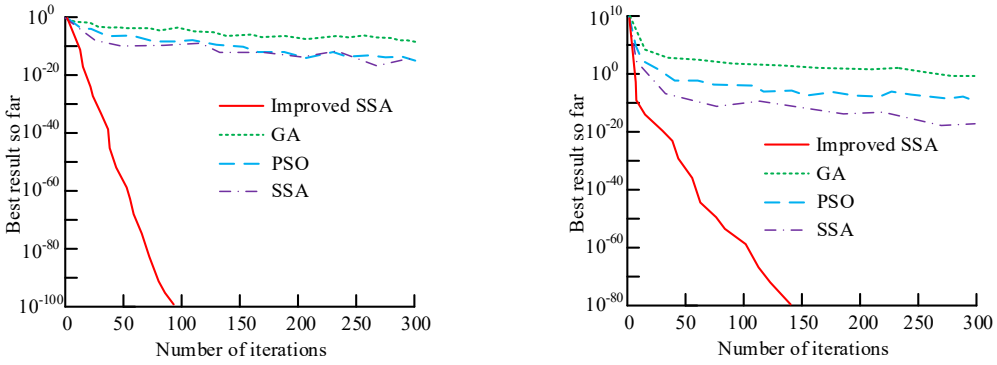

Fig. 6. Optimization results of the ISSA in different single-mode test functions

In Fig. 6(a), the optimization accuracy was defined as the deviation between the objective function value and the theoretical optimum, expressed on a logarithmic scale. The improved SSA achieved optimal optimization accuracy around 90 iterations (mean squared error reduced to 1×10^{-100}), significantly outperforming GA, SSA, and PSO algorithms. The second-best SSA attained optimal optimization accuracy with a mean squared error reduced to 1×10^{-15}. In Fig. 6(b), the decline rate of the improved SSA's curve moderated, achieving optimal accuracy of 1×10^{-80} after 140 iterations. This moderation arose because the F2 test function was nonconvex, resulting in reduced data acquisition by the algorithm. The optimization performance of ISSA across different multimodal test functions is illustrated in Fig. 7.

In Fig. 7(a), the improved SSA demonstrated superior optimization performance on the multimodal test function F3, achieving optimal accuracy after 100 iterations (with the mean squared error reduced to 1×10^{-20}). The second-best SSA achieved an optimal accuracy of 1×10^{0}. In Fig. 7(b), this convergence speed was 50 iterations faster than both the SSA and PSO algorithms, whilst delivering the highest convergence accuracy.

3.2. Emergency Logistics Case Study

The experimental hardware and software configurations remained identical to those in Section 1. The maximum iteration count for the improved SSA was set to 200. The experiment used a real-world pandemic response scenario, based on data

from the 2022 material allocation records publicly released by a provincial epidemic prevention command center. This dataset comprises the actual coordinates, transport costs, and demand data for 4 SPs, 2 warehousing centers, and 10 DPs. The specific structure of the emergency logistics network topology is shown in Fig. 8.

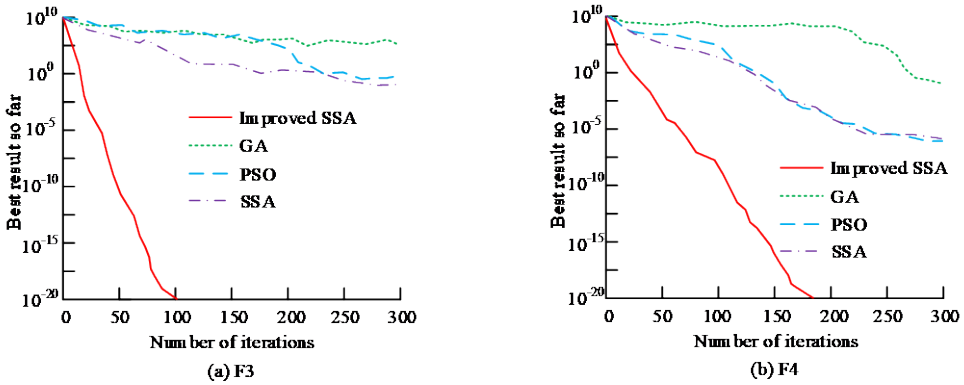

Fig. 7. Optimization results of the ISSA in different multimodal test functions

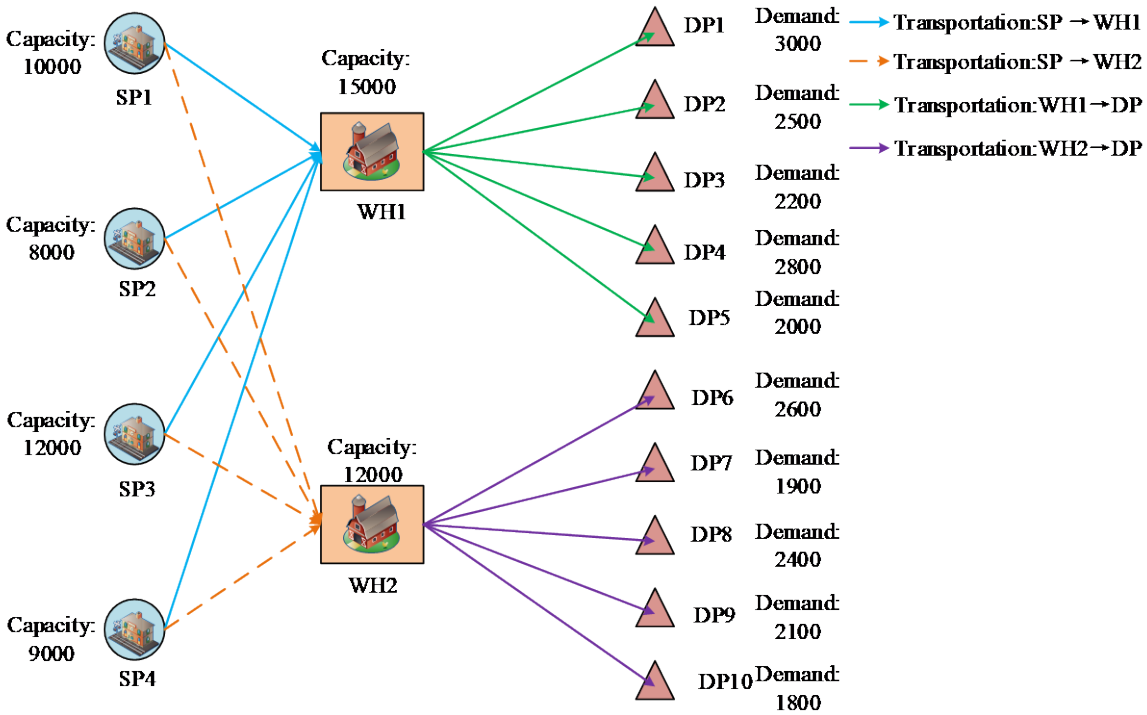

Fig. 8. Emergency logistics network topology diagram

In this logistics network, emergency supplies are first transported from supply points to warehouse centers and subsequently distributed to downstream disaster areas through distribution points. Specifically, SP1-SP4 are responsible for emergency material production and reserve supply. WH1 and WH2 function as regional transshipment and temporary storage centers. DP1-DP10 represent disaster-affected demand areas with different urgency levels. The transportation relationships between nodes are fully connected. For example, SP1 can deliver materials to both WH1 and WH2, while each warehouse center can distribute supplies to all downstream DPs. The transportation cost, transportation time, and interruption probability between nodes are listed in Table 3.

In Table 3, SP1-SP4 represent supply points, WH1 and WH2 are warehousing centers, and DP1-DP10 are DPs. The comparison algorithms employed in this study include SSA, Whale Optimization Algorithm (WOA), and Grey Wolf Optimizer (GWO). The Pareto frontier of ISSA during the MOO of the ELN is displayed in Fig. 9.

In Fig. 9, the distribution of NISs for the ISSA is uniform, with high frontier integrity. The distribution range of NISs for the standard SSA is broader and more dispersed. The emergency logistics command center must make effective decisions between cost and urgency. When a SP suddenly experiences a supply disruption, the emergency adjustment capabilities of different algorithms are shown in Fig. 10.

In Fig. 10(a), the minimum total cost of the improved ascidian algorithm under normal conditions was USD 382,000, and under supply disruption conditions, it was USD 419,000, an increase of only USD 37,000. In contrast, the cost increases

of the whale optimization algorithm, the standard ascidian algorithm, and the grey wolf optimization algorithm were USD 63,000, USD 141,000, and USD 196,000, respectively. This indicated that the improved algorithm was more robust to supply disruptions and could maintain cost efficiency at a near-optimal level. In Fig. 10(b), the minimum total time for the ISSA was 16.5 hours, which was 1.3 hours longer than the uninterrupted run. This increase was 0.6 hours lower than that of the second-best Whale Optimization Algorithm (WOA). The fairness of resource allocation among different algorithms in emergency logistics planning is shown in Fig. 11.

Table 3. Actual Parameters of Some Nodes

Node	Production capacity/ capacity/ demand quantity (pieces)	Cost to WH1 (USD per piece)	Time to WH1 (hours)	Cost to WH2 (USD per piece)	Time to WH2 (hours)	Probability of interruption	Pertinence score
SP1	10,000	5	2	5.8	2.6	0.08	—
SP2	8,000	5.5	2.3	5.2	2.1	0.1	—
SP3	12,000	4.8	2.5	5	2.3	0.12	—
SP4	9,000	5.2	2.2	5.5	2.4	0.09	—
WH1	15,000	—	—	—	—	0.05	—
WH2	12,000	—	—	—	—	0.06	—
DP1	3,000	1.5	1	2	1.3	—	0.92
DP2	2,500	1.6	1.1	1.9	1.2	—	0.85
DP3	2,200	1.4	0.9	2.1	1.4	—	0.78
DP4	2,800	1.7	1.2	1.8	1.1	—	0.71
DP5	2,000	1.5	1	2	1.3	—	0.65
DP6	2,600	1.8	1.3	1.6	1	—	0.6
DP7	1,900	1.9	1.4	1.5	0.9	—	0.55
DP8	2,400	1.6	1.1	1.7	1.1	—	0.5
DP9	2,100	1.7	1.2	1.6	1	—	0.45
DP10	1,800	1.8	1.3	1.5	0.9	—	0.4

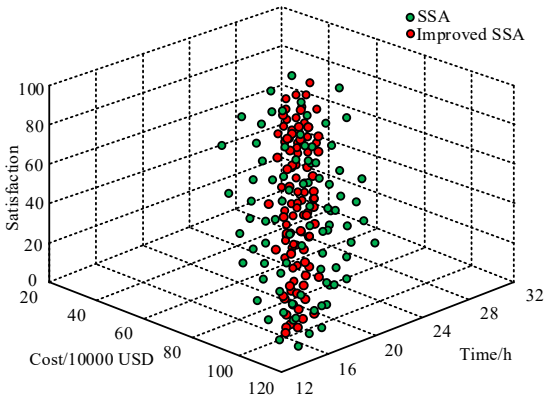

Fig. 9. MOO of ELNs using an ISSA Pareto frontier

In Fig. 11(a), relative unfairness focuses not on absolute quantity differences but on relative proportion disparities. That is, for the same number of resources, the impact of scarcity is far greater for regions with higher demand than for those with lower demand. Under normal conditions without special circumstances, the relative unfairness curves of the four algorithms exhibit similar patterns, all decreasing rapidly between 40 and 120 iterations. The minimum relative unfairness achieved by ISSA was 0.083, which was 0.022, 0.012, and 0.026 lower than those of Grey Wolf Optimizer (GWO), WOA, and SSA, respectively. In Fig. 11(b), shows that when unexpected events occurred, the convergence speed decreased, and relative unfairness increased. The relative unfairness of ISSA increased by 0.015. The ablation experiment results for ISSA are shown in Fig. 12.

In Fig. 12, after removing the nonlinear adaptive adjustment, backpropagation learning, and LF optimization strategies, the ISSA's performance decreased to varying degrees. Furthermore, the convergence position shifted to a later stage. Among these, the algorithm's performance was most significantly impacted by nonlinear adaptive adjustment. Removing this module increased total logistics costs by USD 219,000. Eliminating backward learning and LF increased total costs by USD 95,000 and USD 142,000, respectively. In Fig. 12(b), removing the nonlinear adaptive adjustment increased total transportation time by 1.7 hours. Table 4 compares the computational complexity of several algorithms

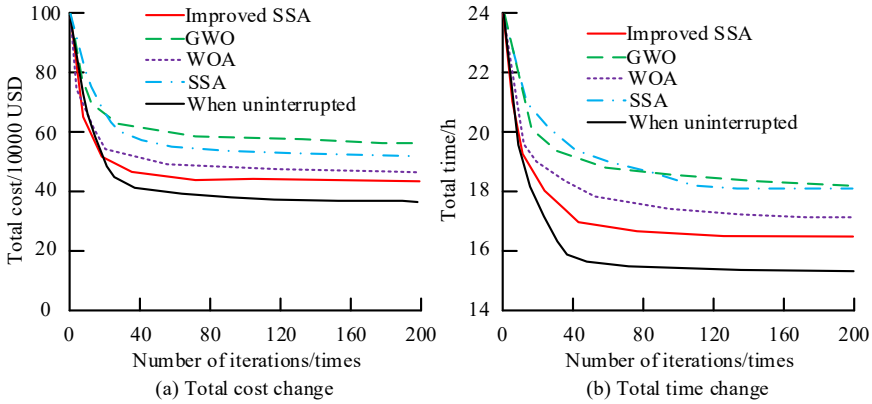

Fig. 10. Emergency adjustment capabilities of different algorithms during supply interruptions

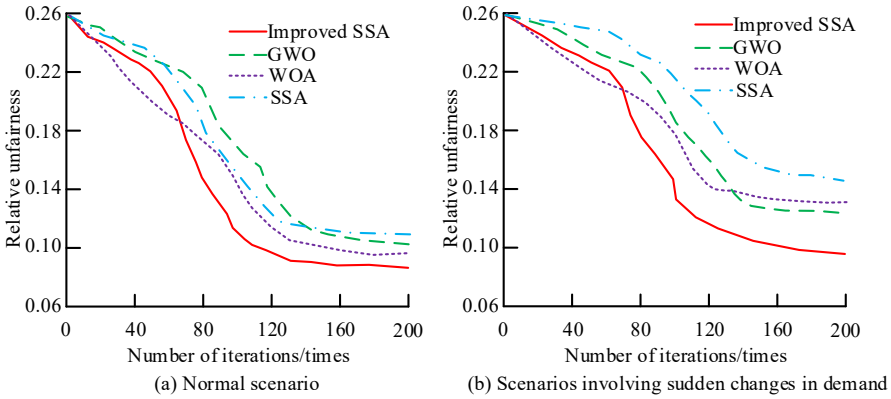

Fig. 11. Fairness of material allocation among different algorithms in emergency logistics planning

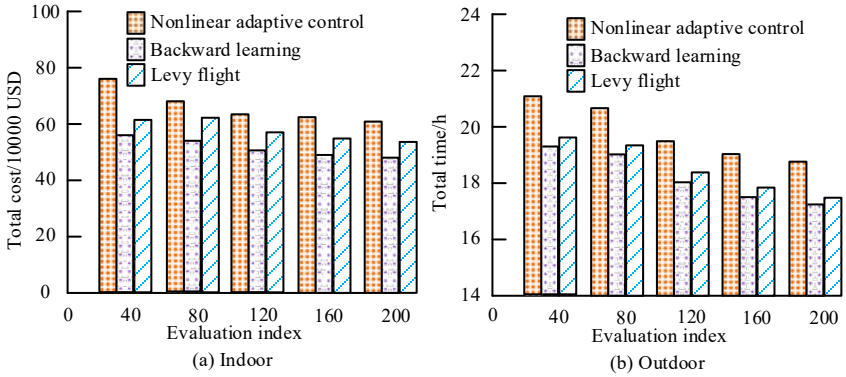

Fig. 12. Ablation experiment results of the ISSA

In Table 4, the proposed ISSA achieved optimal performance, with an algorithm training time of 0.5 hours and a runtime of 57ms. These values were 0.9 hours and 23ms lower than the baseline SSA. The ISSA had 47.2 million parameters, slightly higher than the standard SSA's 35.8 million, but 21.7 million fewer than WOA's 69.9 million. Its floating-point operation count was 92.3 billion, exceeding SSA's by 39.6 billion, while exhibiting lower time complexity. The algorithm performance comparison across different scales is shown in Table 5.

In Table 5, the improved SSA achieved the minimum total cost across different problem scales. As the scale increased from small to large, the standard deviation of the total cost rose from USD 4200 to USD 2100. This remained significantly

lower than the total cost standard deviation for the SSA, which ranged from USD 2940 to USD 12460. The relative unfairness standard deviation of the improved SSA at large scales was 0.004, 0.006 lower than the second-best WOA algorithm, indicating its robust performance. The performance comparison of the improved SSA in earthquake and flood scenarios is shown in Table 6.

Table 4. Comparison of computational complexity of different algorithms

Model	Training time/h	Operating time/ms	Parameter quantity /M	Floating-point operation count /G	Time complexity /O2
ISSA	0.5	57	47.2	92.3	Lower
SSA	1.4	80	35.8	52.7	Normal
GA	3.8	65	40.5	90.5	Lower
PSO	1.1	93	39.5	35.4	Normal
GWO	2.9	109	28.4	58.9	Higher
WOA	1.5	154	68.9	72.5	Higher

Table 5. Comparison of algorithm performance at different scales

Problem Scale	Algorithm	Total cost/Ten Thousand USD	Transportation Time/h	Demand fulfilment rate/%	Relative inequity
(4 supply point/2 warehouses/10 DPs)	Improved SSA	41.9±0.3	16.5±0.2	96.2±0.5	0.083±0.002
	SSA	56.0±2.1	18.2±0.8	88.5±3.2	0.109±0.008
	WOA	48.2±1.5	17.1±0.6	92.1±2.4	0.095±0.006
	GWO	57.8±2.8	19.5±1.2	85.3±4.1	0.125±0.010
(6 supply points/3 warehouses/12 DPs)	Improved SSA	85.6±0.8	24.3±0.4	95.1±0.6	0.091±0.003
	SSA	112.4±4.5	28.9±1.5	84.2±4.8	0.135±0.012
	WOA	98.7±3.2	26.2±1.1	90.3±3.1	0.108±0.008
	GWO	118.9±5.1	31.5±2.3	80.5±5.6	0.152±0.015
(8 supply points/4 warehouses/15 DPs)	Improved SSA	162.3±1.5	35.8±0.7	93.8±0.8	0.105±0.004
	SSA	215.7±8.9	42.6±2.8	79.8±6.3	0.168±0.018
	WOA	185.4±5.8	38.9±2.1	87.5±4.2	0.125±0.010
	GWO	228.6±9.7	46.3±3.5	75.2±7.1	0.189±0.021

Table 6 shows that the earthquake scenario was characterized by concentrated demand, multiple route disruptions, and rapid demand growth. In contrast, the flood scenario features dispersed and changing demand and deteriorating transport routes. The enhanced SSA demonstrated optimal overall performance across both disaster scenarios. In the earthquake scenario, the total cost across all algorithms increased by about 40%. However, the enhanced SSA remained the least expensive at USD 81620, which was USD 9660 less than the second-best WOA algorithm. In the flood scenario, the improved SSA reduced transport time to 19.8 hours, a 3.1-hour decrease compared to the SSA. Furthermore, the improved SSA maintained the lowest relative inequity (0.083-0.095) across all scenarios, demonstrating sound resource allocation fairness. These results fully validated the effectiveness and adaptability of the improved SSA across diverse emergency logistics scenarios. The improved SSA algorithm achieved the highest level of urgency satisfaction in both scenarios. In the earthquake scenario, the urgency satisfaction was 0.08, 0.04, and 0.11 higher than that of the SSA, WOA, and GWO algorithms, respectively. In the flood scenario, the urgency satisfaction was 0.91, which was 0.04 higher than the second-best WOA.

4. Conclusion

This study proposed an emergency logistics planning model employing a multi-strategy ISSA. Experiments demonstrated that the ISSA achieved optimal optimization accuracy of (mean squared error reduced to 1×10^{-100}) after approximately 90 iterations, while the second-best SSA reached an optimal optimization accuracy of 1×10^{-15}. The ISSA exhibited a more uniform distribution of NISs with higher frontier integrity. The command center must make effective decisions balancing cost, investment, and urgency satisfaction. During supply disruptions, total transportation costs increased across all models.

The total cost for ISSA rose by USD 37,000, while GWO, WOA, and SSA saw increases of USD 196,000, USD 63,000, and USD 141,000, respectively. The minimum relative unfairness of ISSA was 0.083, which was 0.022, 0.012, and 0.026 lower than that of GWO, WOA, and SSA, respectively. After removing the nonlinear adaptive adjustment, total logistics costs increased by USD 219,000. In summary, the ISSA effectively accelerates emergency logistics coordination and reduces overall transportation costs. Even when MOO was carried out, the minimum relative unfairness was only 0.083 and never reached the ideal zero value. This revealed an unsettling fact in emergency logistics: under the constraint of limited resources, completely fair distribution is impossible, and managers must accept a certain degree of "necessary injustice". Maximizing the satisfaction of urgency may result in no supplies reaching low-urgency areas, which contradicts the humanitarian principle of "not giving up on any disaster victim". The relative unfairness introduced in this study attempts to balance the two, but where is the optimal balance point, and should a minimum service guarantee level be set in the future? After reading this article, emergency logistics managers should no longer rely on experience to use fixed-weighted summation, but instead dynamically select solutions based on the Pareto frontier at different disaster stages (prioritizing time during the golden rescue period and cost during the reconstruction period); they should no longer distribute supplies equally based on demand, but rather allocate them differently based on the urgency score calculated by entropy weight-TOPSIS, significantly increasing the priority of high-urgency areas (such as areas with a concentration of vulnerable groups); meanwhile, they should use algorithms to simulate supply disruptions, prepare alternative route plans in advance, and embed the improved SALP swarm algorithm into the decision support system to achieve dynamic re-optimization and scheduling every 30 minutes. This study also presents certain limitations, such as the use of static data, which differs from the dynamic information updates encountered in actual rescue scenarios. Future research could incorporate real-time traffic information and demand fluctuations to design an event-triggered, dynamic re-optimization mechanism. Specifically, the system would automatically trigger algorithmic re-planning when the rate of demand change exceeds a threshold or transport routes become disrupted. This mechanism could be integrated with digital twin technology to create a real-time response framework.

Table 6. Performance comparison of the improved SSA in earthquake and flood scenarios

Type of Disaster	Algorithm	Total cost/Ten Thousand USD	Transportation time/h	Demand fulfilment rate/%	Urgency satisfaction	Relative unfairness	Convergence iteration count
Earthquake	Improved SSA	58.3	22.1	94.8	0.89	0.095	55
	SSA	73.5	25.6	86.2	0.81	0.128	140
	WOA	65.2	23.8	90.5	0.85	0.108	95
	GWO	76.9	27.3	82.7	0.78	0.142	170
Flood	Improved SSA	52.7	19.8	95.5	0.91	0.088	48
	SSA	68.4	22.9	87.8	0.83	0.119	130
	WOA	59.6	21.2	91.9	0.87	0.101	85
	GWO	71.2	24.7	84.1	0.79	0.135	160

Author Contributions

Yijia Gao contributed to conception and design, material preparation, data collection, analysis and draft of the manuscript.

Tingfen Gao contributed to the conception, design, manuscript review and revision.

Funding

This research received no specific financial support from any funding agency.

Institutional Review Board Statement

Not applicable.

Declaration of Artificial Intelligence (AI) Tools

The authors used Grammarly Academic solely for language editing and readability improvement. The authors reviewed and verified all content and take full responsibility for the accuracy and integrity of the manuscript.

References

Abed-Alguni, B. H., Paul, D., and Hammad, R. (2022). Improved salp swarm algorithm for solving single-objective continuous optimization problems. *Applied Intelligence*, 52(15), 17217-17236. https://doi.org/10.1007/s10489-022-03269-x

Abideen, A. Z., Sorooshian, S., Sundram, V. P. K., and Mohammed, A. (2023). Collaborative insights on horizontal logistics to integrate supply chain planning and transportation logistics planning-A systematic review and thematic map. *Journal of Open Innovation: Technology, Market, and Complexity*, 9(2), 100066-100082. https://doi.org/10.1016/j.joitmc.2023.100066

Aloui, A., Hamani, N., Derrouiche, R., and Delahoche, L. (2022). Assessing the benefits of horizontal collaboration using an integrated planning model for two-echelon energy efficiency-oriented logistics networks design. *International Journal of Systems Science: Operations and Logistics,* 9(3), 302–323. https://doi.org/10.1080/23302674.2021.1887397

Chen, H., and Cai, Y. (2025). An improved salp swarm algorithm for collaborative scheduling of discrete manufacturing logistics with multiple depots. *International Journal of Autonomous and Adaptive Communications Systems*, 18(1), 1-22. https://doi.org/10.1504/ijaacs.2025.10059647

Chukwuka, O. J., Ren, J., Wang, J., and Paraskevadakis, D. (2023). A comprehensive research on analyzing risk factors in emergency supply chains. *Journal of Humanitarian Logistics and Supply Chain Management*, 13(3), 249-292. https://doi.org/10.1108/jhlscm-10-2022-0108

Dewangan, R. K., and Saxena, P. (2023). Three-dimensional route planning for multiple unmanned aerial vehicles using salp swarm algorithm. *Journal of Experimental & Theoretical Artificial Intelligence,* 35(7), 1059-1078. https://doi.org/10.1080/0952813x.2022.2059107

Ergün, S., Usta, P., Alparslan Gök, S. Z., and Weber, G. W. (2023). A game theoretical approach to emergency logistics planning in natural disasters. *Annals of Operations Research,* 324(1), 855-868. https://doi.org/10.1007/s10479-021-04099-9

Ghasemi, P., Goodarzian, F., and Abraham, A. (2022). A new humanitarian relief logistic network for multi-objective optimization under stochastic programming. *Applied Intelligence,* 52(12), 13729-13738. https://doi.org/10.1007/s10489-024-06174-7

Huang, L. Y., Li, S. Y., Zou, X., Zhao, B. Z., and Li, C. L. (2025). Knowledge-driven logistics transformation: Complex networks and UAVs in distribution. *Journal of the Knowledge Economy,* 16(1), 1583-1622. https://doi.org/10.1007/s13132-024-01984-z

Jalal, A. M., Toso, E. A. V., and Morabito, R. (2022). Integrated approaches for logistics network planning: A systematic literature review. *International Journal of Production Research,* 60(18), 5697-5725. https://doi.org/10.1080/00207543.2021.1963875

Liu, W., Liang, Y., Bao, X., Qin, J., and Lim, M. K. (2022). China's logistics development trends in the post COVID-19 era. *International Journal of Logistics Research and Applications*, 25(6), 965-976. https://doi.org/10.4018/978-1-7998-8856-7.ch012

Mahmood, A. I., Alsaif, O. I., and Saleh, I. A. (2022). Routing flying ad hoc network using salp swarm algorithm. *Indonesian Journal of Electrical Engineering and Computer Science,* 28(2), 946-953. https://doi.org/10.11591/ijeecs.v28.i2.pp946-953

Malik, S., and Suhag, S. (2022). A coordinated control strategy for frequency regulation in hybrid shipboard power system using novel salp swarm algorithm tuned fractional controller. *International Journal of Ambient Energy,* 43(1), 5638-5653. https://doi.org/10.1080/01430750.2021.1973558

Mu, N., Wang, Y., Chen, Z. S., Xin, P., Deveci, M., and Pedrycz, W. (2023). Multi-objective combinatorial optimization analysis of the recycling of retired new energy electric vehicle power batteries in a sustainable dynamic reverse logistics network. *Environmental Science and Pollution Research,* 30(16), 47580-47601. https://doi.org/10.1007/s11356-023-25573-w

Sun, Z., Wang, Q., Chen, L., and Hu, C. (2022). Unmanned technology-based civil-military intelligent logistics system: From construction to integration. *Journal of Beig Institute of Technology,* 31(2), 140-151. https://doi.org/10.1016/j.jii.2023.100534

Tian, G., Lu, W., Zhang, X., Zhan, M., Dulebenets, M. A., Aleksandrov, A., and Ivanov, M. (2023). A survey of multi-criteria decision-making techniques for green logistics and low-carbon transportation systems. *Environmental Science and Pollution Research,* 30(20), 57279-57301. https://doi.org/10.1007/s11356-023-26577-2

Yao, Y., Lei, S., Guo, Z., Li, Y., Ren, S., Liu, Z., and Luo, P. (2023). Fast optimization for large scale logistics in complex urban systems using the hybrid sparrow search algorithm. *International Journal of Geographical Information Science,* 37(6), 1420-1448. https://doi.org/10.6084/m9.figshare.19289150

Zhang, H., Liu, T., Ye, X., Heidari, A. A., Liang, G., Chen, H., and Pan, Z. (2023). Differential evolution-assisted salp swarm algorithm with chaotic structure for real-world problems. *Engineering with Computers,* 39(3), 1735-1769. https://doi.org/10.1007/s00366-021-01545-x

Zhang, Y., Ding, Q., and Liu, J. B. (2022). Performance evaluation of emergency logistics capability for public health emergencies: Perspective of COVID-19. *International Journal of Logistics Research and Applications,* 25(12), 1509-1522. https://doi.org/10.1080/13675567.2021.1914566

Zhou, B. H., and Zhang, J. H. (2023). An improved bi-objective salp swarm algorithm based on decomposition for green scheduling in flexible manufacturing cellular environments with multiple automated guided vehicles. *Soft Computing,* 27(22), 16717-16740. https://doi.org/10.1007/s00500-023-09016-9

Yijia Gao holds a Doctor of Business Administration (DBA) degree. She is currently serving as the Program Leader for Business Enterprise Management at Yunnan Vocational College of Mechanical and Electrical Technology and holds the academic title of Lecturer. Yijia Gao's research has been published in multiple prestigious journals and international conference proceedings. Her academic interests encompass logistics management and machine learning.

Tingfen Gao holds a master's degree in Business Management. She is currently serving as the Examination Administrator at the Academic Affairs Office of Yunnan University of Finance and Economics and holds the academic title of Associate Professor. Tingfen Gao's research has been published in multiple internationally renowned journals. Her academic interests focus on business management and higher education administration.